Applied fault topology: understanding connectivity and uncertainty of fault systems that define and affect commercial and environmental projects

Frank Richards[1]*, Mark Cowgill[1] and Megan Rayner[1].

Abstract

For subsurface commercial ventures or environmental projects that rely on maps of faulted horizons, accurate maps are fundamental. Fault topology provides an ideal tool for analysis of connectivity of fault systems. The data required to undertake the analysis is straightforward to extract from fault maps and can readily be compared to analogue data. In this paper we introduce the concept of fault topology and present existing and new analogue data. To get the most from applying topology the analysis must be coupled with knowledge of the structural history. This includes, the magnitude of faulting, the number of phases of activity and the angle of intersection of successive faulting events. We present a series of case studies that firstly illustrate how topology can capture and define variations in connectivity of fault systems and, secondly, demonstrate how fault topology can be used to identify potential anomalies.

Introduction

Subsurface maps of horizons and the faults that affect them are of fundamental importance to the energy industry. The size, geometry, connected elements and the position of potential barriers is equally important for emerging energies and carbon storage as it is to petroleum accumulations (Stober et al 2017, Mulrooney et al 2020). The application of topology to better understand connectivity in fracture networks has been discussed by Ortega & Marrett (2000) and Sanderson & Nixon (2015). More recently, topology has been applied to fault systems from a variety of data types; outcrop, horizontal seismic sections, seismically mapped horizons, analogue models and remote sensed data (Morley & Nixon 2016, Duffy et al 2017, Morley & Binazirnejad 2020, Mendes et al 2022, Kania & Szczęch 2020, Osagiede et al 2023). In this paper we will briefly review fault topology, but the main objective is to demonstrate how topology can be used to clearly quantify the connectivity of a fault system at a particular level (mapped horizon or unconformity). Also, how topology can be used to spot significant changes in connectivity and how by integrating knowledge of the tectonic setting and structural history it is possible to identify potential errors in the interpretation.

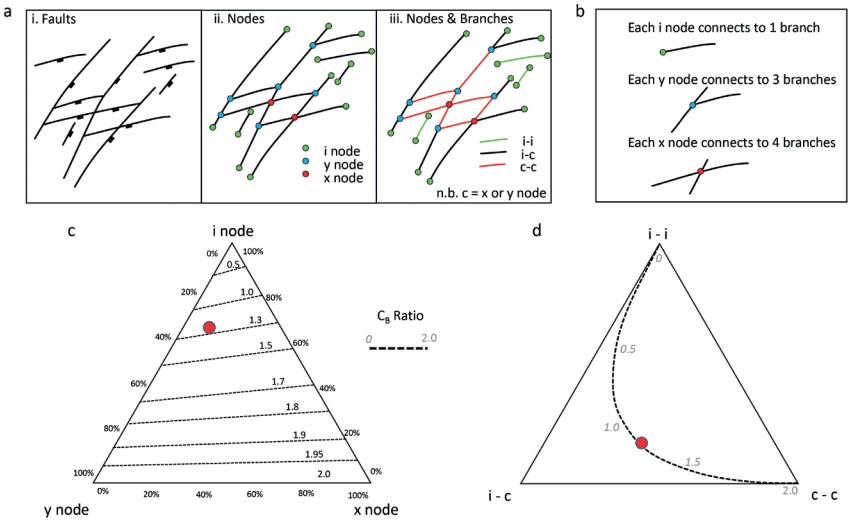

Figure 1 (a) (i) Map showing a population of normal faults (ii) Node types (iii) Branch types (b) Node types with the number of branch connections (c) Fault node topology graph (d) Fault branch topology graph. Both graphs show the C_B ratio as defined by Sanderson and Nixon (2015).

[1] CGG

* Corresponding author, E-mail: francis.richards@CGG.com

DOI: 10.3997/1365-2397.fb2023098

Fault topology

The first step of undertaking topological analysis requires the identification of how the fault elements connect; the size, magnitude of displacement and geometry of the faults are immaterial. Fault terminations (tips) are defined as isolated i-nodes, fault connections as y-nodes and crosscutting faults as x-nodes (Figure 1). Fault branches are the portions of the fault located between nodes. There are three types of fault branch: 'i to i' (isolated), 'i to c' (connected at one end) and 'c to c' (connected at both ends) (Figure 1). The number of branches (N_B) is given by:

$$N_B = ½(N_i + 3N_y + 4N_x)$$

The level of connectivity of a fault system can be expressed in terms of the average number of connections per branch (C_B):

$$C_B = (3N_Y + 4N_X)/N_B$$

The C_B ratio is a dimensionless number between 0 and 2: completely isolated to completely connected (Sanderson and Nixon, 2015). Topology data plotted onto ternary graphs, shows the relative proportions of the different node types (i, y or x) or branch types (i-i, i-c, c-c). In the node topology graph C_B is expressed as a series of contours, in the branch topology graph the ratio plots as a curved line with increasing C_B (Sanderson and Nixon 2015). In both plots, the degree of connectivity increases towards the base of the graph.

In this paper we focus on using fault branch topology, as fault populations – unlike fracture populations – tend to be more binary (i and y nodes) as cross cutting faults evolve with displacement from x nodes to discrete pairs of y nodes and thus cluster along the i-y axis of the node ternary plot (Duffy et al 2017).

Figure 2 shows a set of analogue data derived predominantly from maps of surfaces generated from good quality 3D seismic data. Also included are data from outcrop images and from the results of analogue modelling (Clifton et al 2000, Henza et al 2011). New data presented in this study is also summarised in Appendix 1.

Seismic quality is infinitely variable and can vary greatly even within a single data set. However, to capture as reliable data as possible, we endeavor to use only what we consider to be 'good quality' seismic data. We define 'good quality' seismic as:

i. data with a high signal to noise ratio, i.e., clean data where seismic reflections are clear and faults, for the most part, can be readily identified particularly at the level of interest.
ii. Where faulted, multiple reflectors of the relative upthrown and downthrown seismic sequences can be correlated with a high level of certainty, or in the case of syn-depositional faulting, a growth package can be clearly identified.

For published maps, where there is no (or limited) seismic data available, we include maps that show clear, unambiguous faults and show no anomalous faults with the application of basic structural tests (such as fault displacement – length relationships). Published data from Duffy et al (2017) has also been included in the ternary plot in Figure 2.

Despite the inherent uncertainty in using such a mix of analogue data, the data shows a good fit to the C_B trend line (Figure 2). Analogues from areas subject to just a single phase of extension display low levels of connectivity (e.g., Top Miocene, Bonaparte Basin, Figure 2) and areas where two sets of intersecting faults are present show high levels of connectivity (e.g., Gullfaks field map, Figure 2). These observations are consistent with published studies where topology has been applied (Morley & Nixon 2016, Duffy et al 2017, Morley & Binazirnejad 2020). In essence we have the makings of a consistent theoretical and analogue-based framework which can be used to evaluate maps which, for example, were generated from poor quality data, where there is limited coverage or where there may be a viable alternate interpretation.

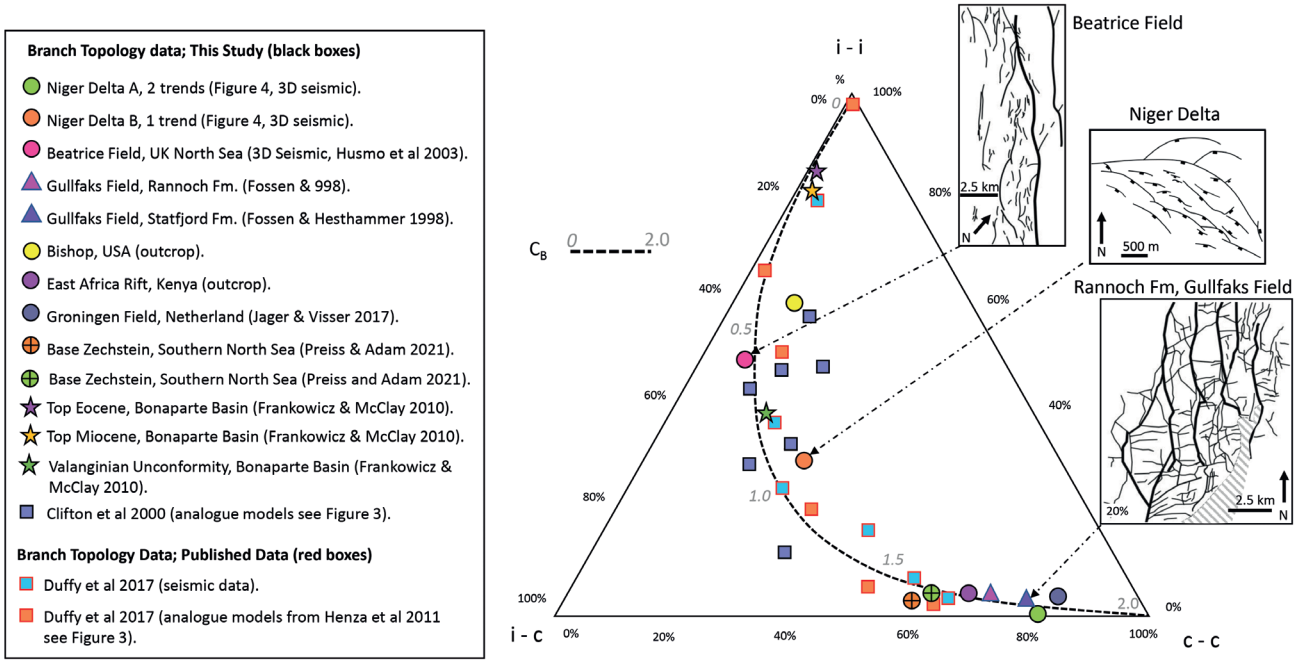

Figure 2 Fault branch topology plot of analogue data.

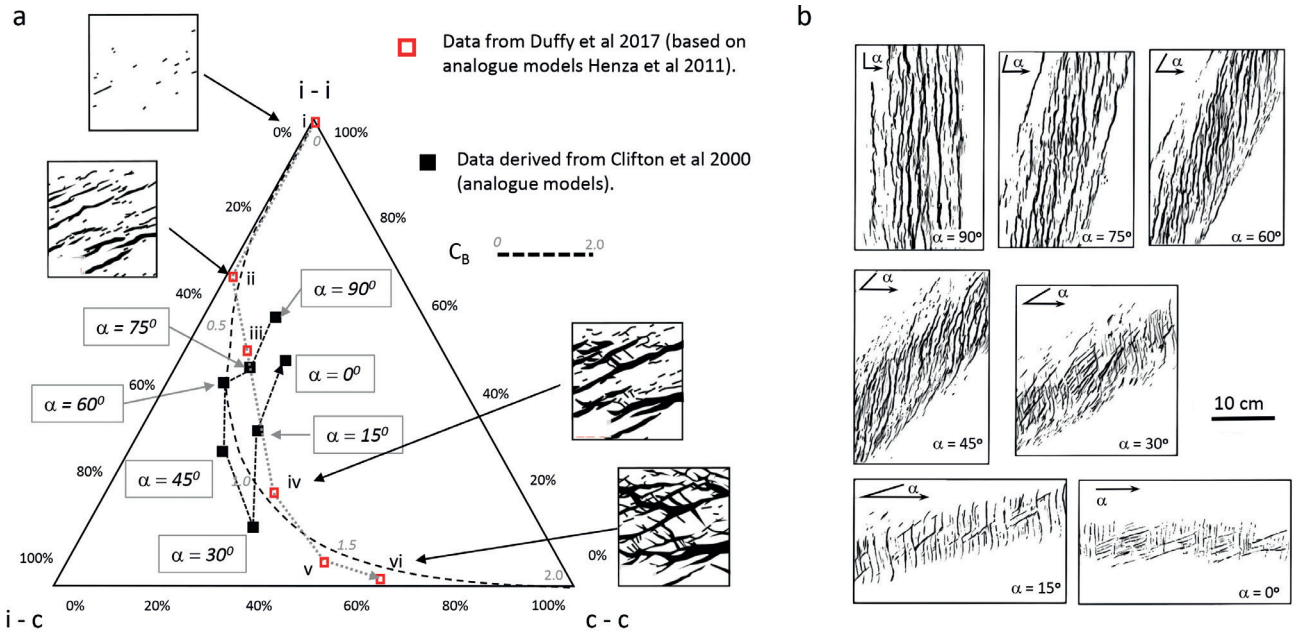

Figure 3 Fault branch topology data derived from physical models (a) Open red squares; data from Duffy et al (2017) (based on Henza et al 2011). Multi-phase rifting; i to iii = increasing single phase strain, iv-vi = increasing superimposed oblique strain (small inset maps show the detail of the fault patterns at selected stages). Black squares; derived from Clifton et al (2000). α is the angle between a pre-existing structural trend and the angle of the imposed extension in each model. (b) Adapted finite fault maps from Clifton et al (2000) showing the angle α and the position of faults for seven experimental models.

Duffy et al (2017) generated topology data from the analogue clay models of Henza et al (2011) that investigated the nature of faulting associated with two superimposed, oblique extensional faulting events. One of the principal conclusions was that increasing connectivity (C_B) could be correlated with increasing strain along a single fault trend for low ratios (C_B = 0 – 0.8) and that higher ratios (C_B = 0.8 – 2) could only be achieved by having progressively greater movement during a second phase of crosscutting faults (Figure 3). The magnitude of the two events is important, if one of the events is weak, fault connectivity will be limited. The above enhances the potential insights that fault topology may provide. In that, knowledge and understanding of the geological history of a region can be cross-referenced with the graphical representations on the ternary plot.

Figure 3 also shows topology data generated from a suite of physical models undertaken by Clifton et al (2000). In these experiments a layer of clay was subject to a single phase of extension orientated at variable angles with respect to an underlying rift trend (angle α). The modelling and finite extension was very similar to that of Henza et al (2011). The geometry of the rift axis was controlled by overlapping steel plates overlain by a latex sheet. The results showed that when extension was orthogonal ($\alpha = 90^0$) or at a high angle (down to $\alpha = 60^0$) to the direction of the rift, the resulting connectivity was broadly similar to a high strain single phase rift in the experiments of Henza et al (2011). As the angle decreased the connectivity increased significantly to a maximum C_B ratio of 1.25 when α was equal to 30^0 (Figure 3). At very low angles ($\alpha = 15^0$ and 0^0) the connectivity rapidly decreased. It should be noted that two data points plot some distance from the C_B ratio line in the ternary plot ($\alpha = 0^0$ and 90^0), the overall trend is, however, clear. The significance of this is a discussion point later in the paper.

These results suggest that some caution is required in the transition zone between single and multiphase rifts (around C_B 0.8 to 1.25) and we can't automatically assume two phases of faulting. It's possible that a single trend is being affected by, and interacting with, an underlying pre-existing trend. These data also suggest that where there are two phases of extension the angle between the phases is an important factor and needs to be considered.

Case studies

In the next section we will look at a series of contrasting case studies to see how topology can be applied to aid the understanding of connectivity in subsurface maps.

Case Study 1: Niger delta extensional fault system

This relatively simple case study looks at faults that have been mapped on high-resolution 3D seismic data (Figure 4a). The maximum displacement on these faults is low (tens of metres) and the faults shown were derived from a mapped surface. To the southwest of the map a single trend is observed. Despite a high proportion of isolated faults there are areas where some larger faults are well connected. The curved nature of these faults has enhanced the connectivity (C_B ratio around 0.9) (Figure 4b). To the northeast, the presence of a second crosscutting fault trend can be linked to a significant jump in the connectivity with a C_B ratio of around 1.8 (Figure 4b).

This example is a good analogue, it shows how fault topology can be used to quantify changes in fault connectivity on a subregional scale. This is important if we want to apply this methodology, say, on variation that may occur across a producing oil field. The resolution of the data and identifying changes in the fault population (additional faults and changing patterns of strain) are the key factors in this analytical method.

Case study 2: Passive margin extensional fault system

This case study represents the opposite end of the spectrum with regards to data quality; the quality in this case was very poor. The tectonic setting was well understood and along strike analogues, based on better-quality seismic lines, show crustal scale normal faults with kilometre scale displacements. The presence of large-scale transfer zones has also been recognised (linked to pre-existing structural trends) on a regional scale (Figure 5a). The mapped fault population contains a very high proportion of unconnected faults and plots at the top of the ternary diagram (C_B = 0.15, Figure 5b). Populations that plot in this zone are associated with very low strain and with a single set of faults (Figure 3). As we are in a position where we know something about the regional setting, we can feed our understanding of the fault topology into the interpretation: we would expect a high strain rift and the presence of transfer zones to possess a much higher C_B ratio (Figures 2 and 3) (Duffy et al 2017). The ratio of branches to connected nodes, in this case, is far too low. Of course, this approach does not inform us as to which faults may need to be modified, but it does give licence for the interpreter to be much more assertive with the mapping and structural model. In studies with challenging data sets, such feedback is extremely valuable and can significantly improve the quality of the interpretation. It may also prevent a region from being written off and make it easier to push ahead and acquire new data.

Case study 3: Multiple models

This case study considers multiple alternative interpretations of an identical data set. It highlights the inherent uncertainty associated with interpreting when there are data issues. In this instance, it was data coverage rather than seismic quality that was the source of the problem. The data was comprised of good quality 2D seismic. Faults imaged on individual lines were clear and consistently identified by the different teams working on the

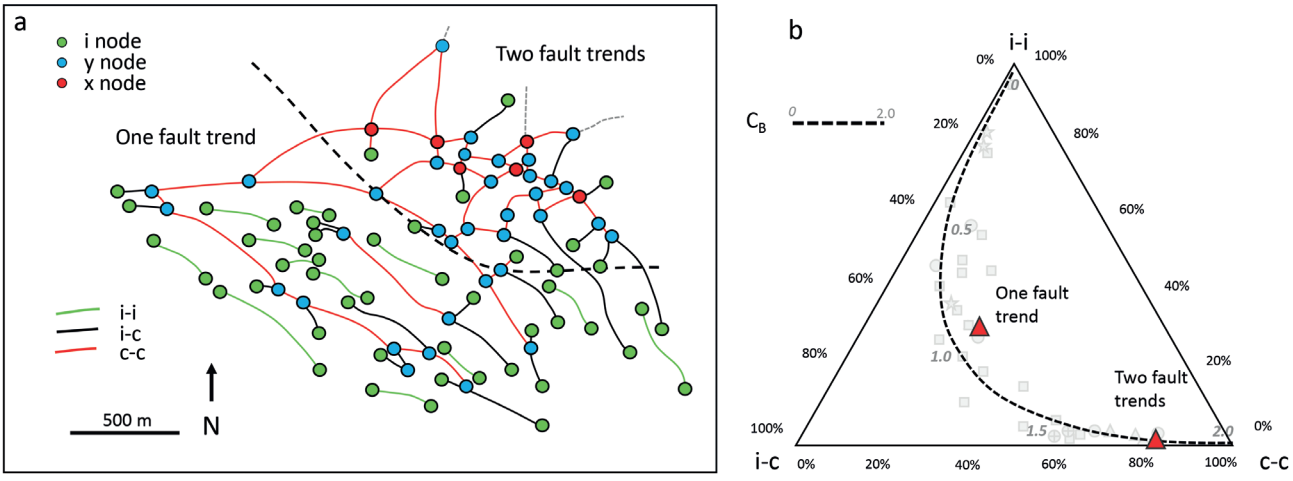

Figure 4 Case Study 1: (a) Fault branch topology map of faulting affecting a shallow surface in the Niger Delta. (b) Fault branch topology plot showing two structural domains. Plot includes data from Figure 2 (grey points).

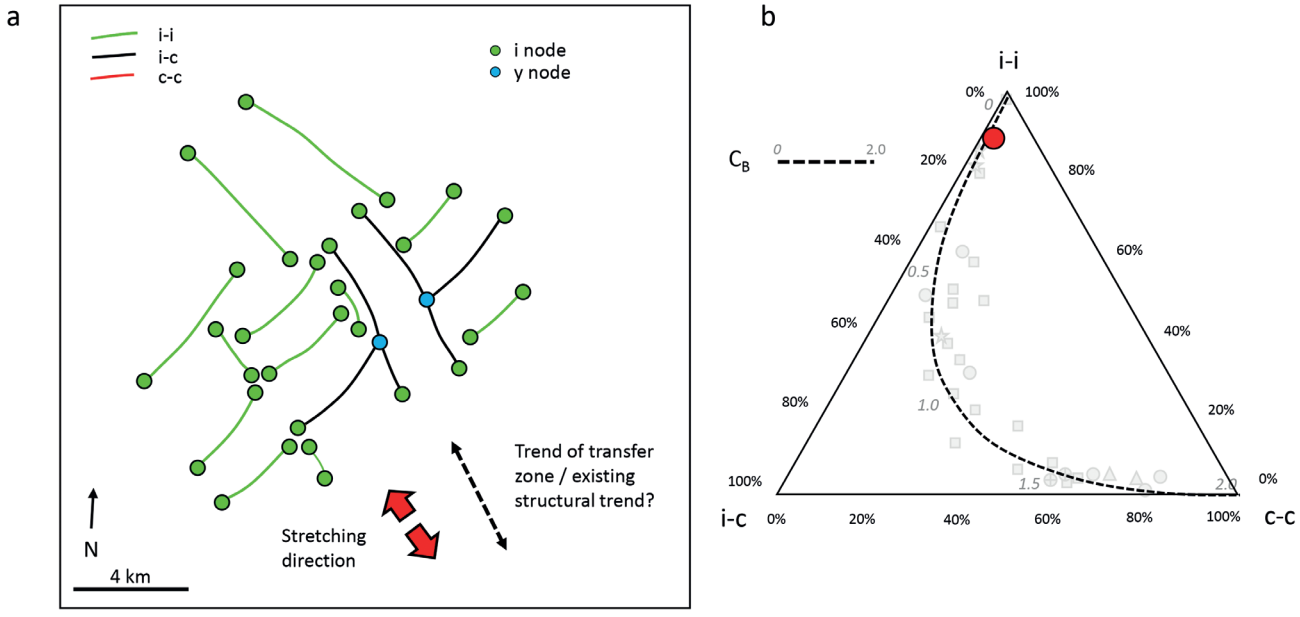

Figure 5 Case Study 2: (a) Fault branch topology map of faults interpreted in a mature passive margin (a surface towards the top of the pre-rift sequence) (b) Fault branch topology graph of the faults in map 5(a). Plot includes data from Figure 2 (grey points).

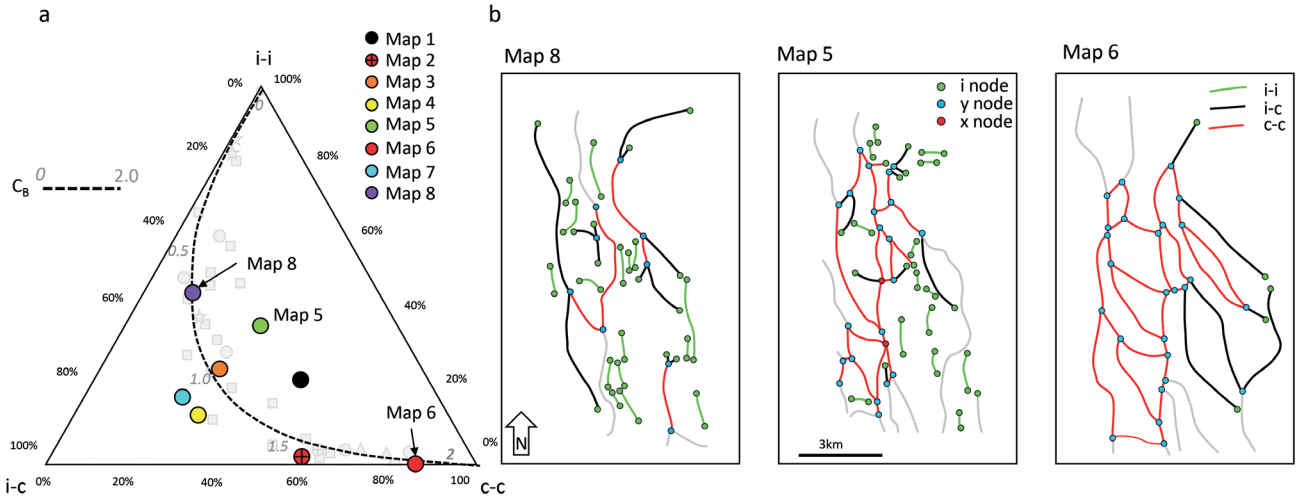

Figure 6 Case Study 3: (a) Fault topology plot based on data collected from eight alternate interpretations of the same 2D seismic data set. Plot includes data from Figure 2 (grey points). (b) Fault branch topology maps.

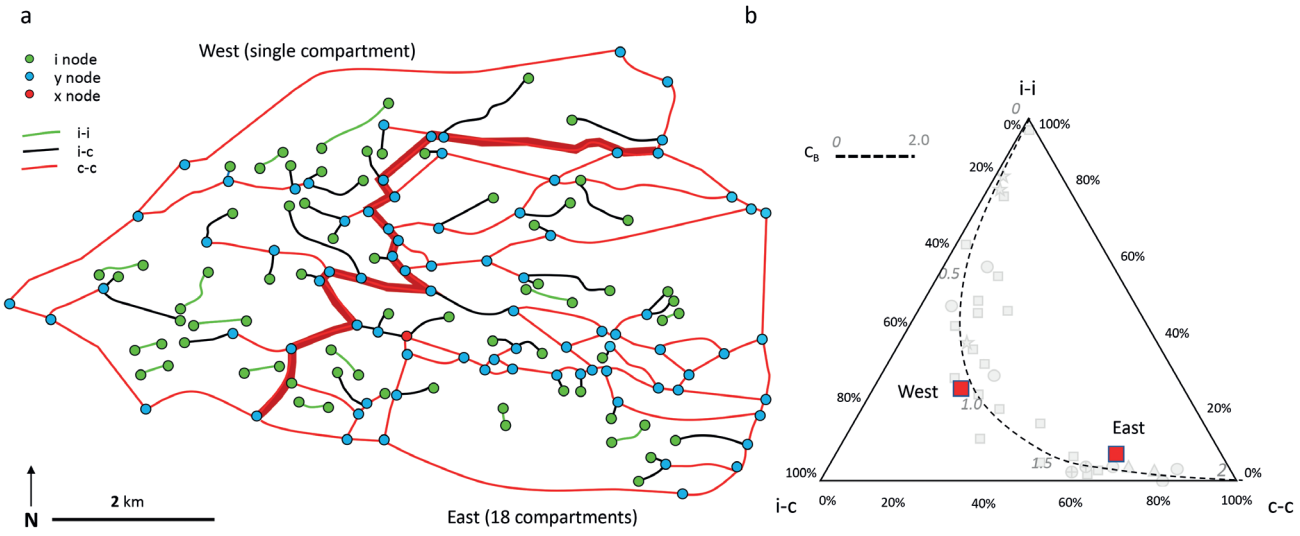

Figure 7 Case study 4: (a) Fault Branch topology map of the Buchan Field, the thick continuous red line separates the uncompartmentalised west from the highly compartmentalised east (adapted from Marshall & Hewett (2003) (b) Fault branch topology plot. Plot includes data from Figure 2 (grey points).

data (Richards et al 2015). How each team chose to link together the faults led to the production of a suite of very different maps (Figure 6). Figure 6a shows the fault branch topology of eight maps included in the study. The alternate maps show a surprising amount of variation with regards to connectivity, with C_B ratios ranging from as low as 0.7 up to 1.8. Three of the maps are shown in Figure 6b, Maps 8 and 6 represent the end members in terms of their fault connectivity; Map 6 was compiled without a single isolated fault, and although Map 8 displays faults with similar trends, 46% of the faults are isolated (Figure 6a). Regardless of the intended use of these two maps, be it defining containers or predicting the movement of fluids, these two maps exhibit radically different scenarios. For example, it's possible to navigate in a north-south direction through the centre of Map 8 without encountering a single fault barrier (Figure 6b).

Can we do more? Can we look at these results and use topology to suggest that some maps are better representations of the subsurface? If we consider the tectonic setting, some of the interpretations appear less likely. The extensional strain at this level is relatively low and although the faults are curved, they generally strike in a north-south direction. There is also evidence of fault reactivation but no change in the direction of extension. Based on this, one could argue that maps that display connectivity close to 2 are unlikely (this would affect two of the eight maps). Although it has yet to be established whether a significant departure from the dashed C_B line in the ternary branch topology graph represents an anomalous map, two of the maps sit significantly outboard of the analogue data (see discussion). So, with comparatively little effort and expenditure we can seriously question four of the eight maps. At the very least these interpretations should be rigorously checked, and additional analysis undertaken (Richards et al 2015).

This case study illustrates the human element of the interpretation process and shows it's possible to generate results covering greater than 50% of the total range of connectivity (C_B 0.7 to 1.8) from identical data. A further conclusion is that anyone using 2D data to define fault patterns for faulted horizons should be very cautious and probably review the implications of alternate scenarios.

Case Study 4: The Buchan Field

The Buchan Field produces from Upper Devonian to Lower Carboniferous reservoirs and is located in the UK North Sea. Early maps, based on 2D data, were comparatively simple and showed the field to be comprised of four fault-bounded compartments (Edwards 1991). For this study an analysis of a more recent map based on 3D data was undertaken (Marshall & Hewett 2003, Figure 7a). It should be noted that the quality of the 3D seismic was comparatively poor (Marshall & Hewett 2003). A topology assessment revealed a potential anomaly in the fault interpretation. The eastern portion of the field is heavily compartmentalised by faults (18 compartments). In stark contrast, a similar-sized area to the west is comprised of a single irregular compartment (Figure 7, a red line defines the boundary between the compartmentalised east and open west). The fault topology from the western side has a C_B ratio of 0.9. The connectivity of the eastern half of the field is predictably much higher (C_B ratio around 1.7, Figure 7b). Case study 1 (Figure 4) showed an example of a rapid variation in connectivity where a new fault trend locally develops and crosscuts an existing trend. Could this be happening across the Buchan Field and was it missed during the interpretation of the 2D data? The regional structural trend is dominated by sub east-west trending faults and intersecting north-south faults have been described by Zanella and Coward (2003). So, it's feasible that north-south faults may be affecting the eastern half of the field but not the west. Two observations suggest this is not the case: the irregular geometry of the transition and the fact that the nature and trends of faults across the whole map, for the most part, are similar. Seemingly, the only difference is that the eastern half is just more connected. As the seismic data is relatively poor, we would argue that the origin of the variation is more likely to be related to how the data was interpreted. Is it possible we are dealing with a merged interpretation? Regardless of the origin of the variation, the analysis strongly suggests that the field needs to be remapped and the connectivity made more consistent.

Case Study 5: The Scott Field

The final case study is based on the fault topology of the Scott Field, which is also located in the UK North Sea. The 3D seismic data that covers the field is generally of good quality. The structure varies in complexity: to the southeast, a single set of northwest-southeast rotated fault blocks are observed, to the west they merge and intersect with a second trend running roughly northeast-southwest (Brook et al 2010). Where the two fault sets are present, the structure is more complex. Numerous intra block faults, with variable orientations are also observed. The strain on all the major faults is high with throws of more than 1000 m. It should be noted that in areas where the complexity is high, the quality of the data is somewhat reduced.

The fault topology analysis shown in Figure 8a is based on faults from within the structural zones defined by master faults (zones A-E, Figure 8b, n.b. the map upon which these data were derived is not shown here), it includes faults that splay or intersect with the larger, block-defining, faults. The connectivity is highly variable but a consistent pattern is evident. Blocks A and B are located where a single fault trend dominates and accordingly displsys lower values of connectivity (C_B 0.5 – 0.8). Blocks C and D, in the more complex area to the NW show higher values of C_B (1.4 to 1.8). The topology of Block E is anomalous: despite lying in the more structurally complex part of the field the connectivity is relatively low with a C_B of around 0.75 (Figure 8a).

Fault topology in this case study was used to recommend revisiting this zone and reassessing the fault interpretation.

Conclusions

When generating subsurface fault maps, with the exception of simple structures illuminated completely by good quality data, uncertainty is a critical issue. The degree of fault connectivity is one of the key uncertainties. The application of fault topology allows us to quantify connectivity and critically, enables us to compare the areas of economic importance to analogues. Case Study 1 represents a good analogue, the quality of the data is very good and there is a high certainty as to how the faults connect. It demonstrates how there can be a rapid transition of fault connectivity over a relatively short distance (Figure 4). The second case study (Figure 5) lies at the opposite end of the

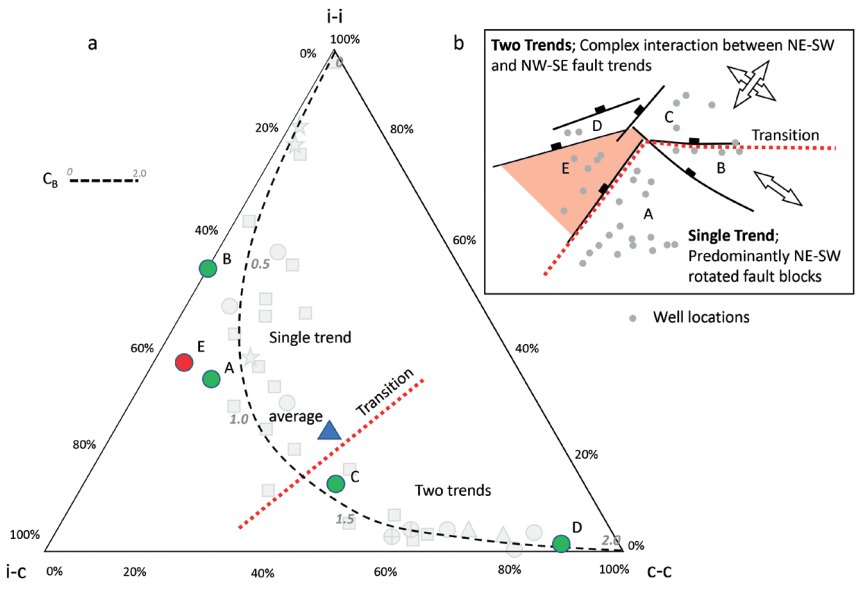

Figure 8 Case study 5: (a) Fault branch topology of intra-block faults of the Scott Field. Points A to E represent data from structural subregions shown in the inset map, *n.b. the data shown on the ternary plot is based on proprietary data that is not shown here.* Plot includes data from Figure 2 (grey points). (b) Simplified map of the Scott Field showing the position of the major faults and intra block subregions A to E. Grey Circles show the position of production wells (adapted from Brook et al 2010).

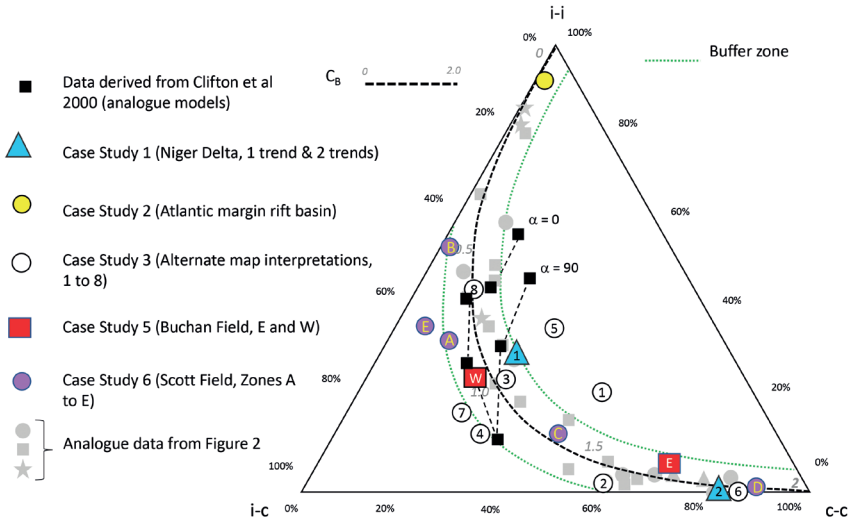

Figure 9 Fault branch topology plot showing an amalgamation of analogue data (in grey), case study data and data from the models of Clifton et al (2000). The plot also shows a 'buffer zone' which runs parallel to the C_B ratio line and bounds the analogue data from Figure 2.

spectrum with regards to mapping uncertainty being based on very poor quality seismic. In this case fault topology can act as a guide, given the understanding of the tectonic setting (a high strain rift margin, with transfer zones) faults were under connected. This gives licence to the interpreter to be more assertive and introduce more connected faults into the interpretation. Case study 3 is a good reminder of the amount of variation inherent in making interpretations. It's also a reminder that the origin of variation is not necessarily about seismic quality, but also about data coverage and the limits of using 2D data (Richards et al 2015). Fault topology was able to identify outliers based on a basic understanding of the regional geology and by comparison with analogue data. In case studies 4 and 5, fault topology was able to quantify the connectivity of structural domains and, by integrating an understanding of the structural geology, help to identify potential anomalies.

Several methods of integrated structural analysis have been available for a number of decades. Commonly applied techniques include cumulative frequency of fault length (and fault displacement) and the ratio of fault displacement with respect to length (Walsh & Watterson 1988, Walsh & Watterson 1992). Freeman et al (2010) demonstrated how the distribution of strain along faults could be used to identify structural anomalies. Other relationships have also been identified, for example the relationship between the magnitude of displacement and width of relay ramps to help predict the probability of ramp breaching (Imber et al 2004). Fault topology offers something new, as it deals directly with fault connectivity. It's also possible for it to be applied directly to lineaments observed on horizontal slices through seismic data (Morley & Nixon 2016), so it can be applied before, or during a mapping exercise.

Discussion: Topology as a QC tool?

The case studies described in this paper show how topology can effectively be deployed to quantify variations in connectivity of fault populations observed on maps. From a QC perspective this alone makes it a useful tool. When integrated with structural geology it is much more powerful. Duffy et al (2017) showed that increasing connectivity (C_B ratio) could be related to increasing strain and multi-phase fault evolution. However, there is still considerable work required to fully understand the evolution of connectivity. For example, data generated from the analogue models of Clifton et al (2000) show how pre-existing trends may enhance connectivity during a single phase of extension. The implication is that it may be difficult in some settings and at certain ratios (around C_B 0.8 to 1.25) to distinguish between single and multi-phase rifting from topology alone.

The C_B ratio line in fault branch ternary plots (Sanderson and Nixon 2015) is mathematically defined 'from randomly assigned node types to branches, weighted by probabilities of occurrence' (Morley and Binazirnejad 2020). Fault topology analogue data presented here (Figure 2) displayed a clear tendency to cluster close to the C_B line (Figure 9). This tendency is also evident in the published data of Duffy et al (2017), Mendes et al (2022) and Osagiede et al (2023). Some data, however, plots away from the line (Figure 9). Some of the published data from Morley and Nixon (2016) and Morley and Binazirnejad (2020) also shows this tendency. It's possible this may be related to geology, it's also possible that it may be linked to the quality of the interpretations, or indeed, some combination of the two. Clearly not all the maps in case study 3 (Figure 6) represent accurate representations of the subsurface. Maps 1 and 5 lie some distance off the C_B ratio line; we propose that this is used as a possible quality flag. We define a buffer zone that bounds the outer limit of the analogue data in Figure 2 and treat data located outside the zone as 'potentially poor' (Figure 9). As more analogue data becomes available and these relationships become better understood, this approach will almost certainly need to be adapted.

With time we predict that the use of fault topology will become increasingly routine and form an important part in any structural QC or review process.

Acknowledgements

We would like to thank the anonymous reviewer for feedback that greatly improved the direction and quality of this paper. Thank you CNOOC for allowing us to use data derived from their map of the Scott Field. We would also like to thank Nick Richardson and Marguerite Fleming for the usual feedback and encouragement.

Map	Data type / quality	Short structural description	Reference / Figure used
Niger Delta A	3D seismic / good	Two intersecting fault trends	N/A Propriety seismic data
Niger Delta B	3D seismic / good	Single Fault Trend	N/A Propriety seismic data
Beatrice Field	3D seismic / good to fare	Single fault trend 2002	Husmo et al (), Figure 10.31a
Gullfaks Field, Rannoch Fm.	3D seismic / good to fare	Single event high strain extensional faults with oblique intra-block faulting	Fossen & Hesthammer (1998), Figure 3
Gullfaks Field, Statfjord Fm.	3D seismic / good to fare	Single event high strain extensional faults with oblique intra-block faulting	Fossen & Hesthammer (1998), Figure 4
Bishop, USA	Satellite image / good outcrop	Single fault trend, low strain	Iny County, California, USA (GR 37.458804, _118.448992)
East Africa Rift, Kenya	Satellite image / good outcrop	Dominant N-S trend affected by localized oblique faulting	Esonorua, Kenya (GR -1.35751, 36.339892)
Groningen Field, Holland	3D seismic / good to fare	Multiple intersecting fault trends	Jager & Visser (2017), Figure 5
Base Zechstein, Southern North Sea	3D seismic / ant tracking, Good	Multiple intersecting fault trends	Preiss and Adam (2021), Figure 7A
Base Zechstein, Southern North Sea 2	3D seismic / ant tracking, good	Multiple intersecting fault trends	Preiss and Adam (2021), Figure 7B
Top Eocene, Bonaparte Basin Australia	3D seismic, ant tracking / good	Single fault trend	Frankowicz, E. and McClay (2010), Figure 8d
Top Miocene, Bonaparte Basin, Australia	3D seismic, ant tracking / good	Single fault trend	Frankowicz, E. and McClay (2010), Figure 8d
Valanginian Unconformity, Bonaparte Basin, Australia	3D seismic / good	Two fault trends	Frankowicz, E. and McClay (2010), Figure 8d
Faults from physical models	Clay analogues models / good image quality	Variable depending on the model; single trend to two crosscutting trends	Clifton et al (2000), Figure 3

Appendix 1 Details of data used to populate the fault branch topology plot in Figure 2.

References

Brook, G.R., Wardell, J.R., Flanagan, S.F. and Regan, T.P. [2010]. The Scott Field: revitalization of a mature field. *Geological Society, London, Petroleum Geology Conference Series*. **7**, 387-403.

Clifton, A.E., Schlische, R.W., Withjack, M.O. and Ackermann, R.V. [2000]. Influence of rift obliquity on fault-population systematics: results of experimental clay models. *Journal of Structural Geology*, **22**(10), 1491-1509.

Cowie, P.A. and Scholz, C.H. [1992]. Displacement-length scaling relationship for faults: data synthesis and discussion. *Journal of Structural Geology*, **14**(10), 1149-1156.

De Jager, J. and Visser, C. [2017]. Geology of the Groningen field–an overview. *Netherlands Journal of Geosciences*, **96**(5), s3-s15.

Duffy O.B., Nixon C.W., Bell R.E., Jackson C A.L, Gawthorpe R.L., Sanderson D.J. and Whipp P.S. [2017]. The topology of evolving rift fault networks: Single-phase vs multi-phase rifts. *Journal of Structural Geology*, **96**, 192-202.

Edwards, C.W. [1991]. The Buchan Field, Blocks 20/5a and 21/1a, UK North Sea. *Geological Society, London, Memoirs*. **14**, 253-259.

Fossen, H. and Hesthammer, J. [1998]. Structural geology of the Gullfaks field, northern North Sea. *Geological Society, London, Special Publications*, **127**(1), 231-261.

Frankowicz, E. and McClay, K.R. [2010]. Extensional fault segmentation and linkages, Bonaparte Basin, outer North West Shelf, Australia. *AAPG Bulletin*, **94**, No.7 977-1010.

Freeman, B., Boult, P.J., Yielding, G. and Menpes, S. [2010]. Using empirical geological rules to reduce structural uncertainty in seismic interpretation of faults. *Journal of Structural Geology*, **32**, 1668-1676.

Husmo, T., Hamar, G.P., Høiland, O., Johannessen, E.P., Rømuld, A., Spencer, A.M. and Titterton, R. [2003]. Lower and middle Jurassic. The Millennium Atlas: Petroleum Geology of the Central and Northern North Sea. *Geol. Soc. London*, 129-156.

Henza, A.A., Withjack, M.O. and Schlische, R.W. [2011]. How do the properties of a pre-existing normal-fault population influence fault development during a subsequent phase of extension? *Journal of Structural Geology*, **33**(9).

Imber, J., Tuckwell, G.W., Childs, C., Walsh, J.J., Manzocchi, T., Heath, A.E., Bonson and Strand, C.G J. [2004]. Three-dimensional distinct element modelling of relay growth and breaching along normal faults. *Journal of Structural Geology*, **26**(10). 1897-1911.

Kania, M. and Szczęch, M. [2020]. Geometry and topology of tectonolineaments in the Gorce Mts. (Outer Carpathians) in Poland, *Journal of Structural Geology* **141**. 104186.

Manzocchi, T. [2002]. The connectivity of two-dimensional networks of spatially correlated fractures. *Water Resources Research* **38**, 1162.

Marshall, J.E.A. and Hewett, A.J. [2003]. Devonian. *The Millennium Atlas: Petroleum Geology of the Central and North Sea*. Geol. Soc. London.

Mendes, L de C., Correia U.M.C., Cunha O.R., Oliveira F.M. and Vidal, A.C. [2022]. Topological analysis of fault network in naturally fractured reservoirs: A case study from the pre-salt section of the Santos Basin, Brazil, *Journal of Structural Geology*, **159**. 103930

Morley C.K. and Binazirnejad H. [2020]. Investigating polygonal fault topological variability: Structural causes vs image resolution, *Journal of Structural Geology*, **130**. 103930.

Morley, C.K. and Nixon, C.W. [2016]. Topological characteristics of simple and complex normal fault networks, *Journal of Structural Geology*, **84**. 68-84.

Mulrooney, M.J., Osmond, J.L., Skurtveit, E., Faleide, J.I. and Braathen, A. [2020]. Structural analysis of the Smeaheia fault block, a potential CO_2 storage site, northern Horda Platform, North Sea. *Marine and Petroleum Geology* **121**.

Nicol, J., Watterson, J., Walsh, J.J. and Childs, C [1996]. The shapes, major axis orientations and displacement patters of fault surfaces, *Journal of Structural Geology*, **18**, 235-248.

Ortega, O. and Marrett, R. [2000]. Prediction of microfracture properties using microfracture information Mesaverde Group sandstones, San Juan Basin, New Mexico. *Journal of Structural Geology,* **22**(5), 571-588.

Osagiede, E.E., Nixon, C.W., Gawthorpe, R., Rotevatn, A., Fossen, H., A-L. Jackson, C., and Tillmans, F. [2023]. Topological characterisation of fault network along the northern North Sea rift margin. *Tectonics*, e2023TC007841.

Preiss, A.D. and Adam, J. [2021]. Basement fault trends in the Southern North Sea Basin. *Journal of Structural Geology*, **153**, 104449.

Richards, F.L., Richardson, N.J., Bond, C.E. and Cowgill, M. [2015]. Interpretational variability of structural traps: implications for exploration risk and volume uncertainty. *Geol. Soc. of London, Special Publications* **421**, 7-27.

Sanderson, D.J. and Nixon, C.W. [2015]. The use of topology in fracture network characterization. *Journal of Structural Geology*, **72**, 55-66.

Stober, I., Fritzer, T., Obst, K., Agemar, T. and Schulz, R. [2017]. Deep Geothermal Energy: Principles and Application Possibilities in Germany. *Federal Ministry for Economic Affairs and Industry.*

Walsh, J.J. and Watterson, J. [1988]. Analysis of the relationship between displacements and dimensions of faults. *Journal of Structural Geology*, **10**(3), 239-247.

Walsh, J.J. and Watterson, J. [1992]. Populations of faults and fault displacements and their effects on estimates of fault-related regional extension. *Journal of Structural Geology*, **14**(6), 701-71.

Zanella, E. and Coward, M.P. [2003]. Structural framework. Chapter 4, *The Millennium Atlas: Petroleum Geology of the Central and North Sea.* Geol. Soc. London.